Journal of Biomechanics 125 (2021) 110598

Contents lists available at ScienceDirect

Journal of Biomechanics

journal homepage: www.elsevier.com/locate/jbiomech

Understanding the effect of window length and overlap for assessing sEMG in dynamic fatiguing contractions: A non-linear dimensionality reduction and clustering

Carlos De la Fuente [a,b,c,d], Eduardo Martinez-Valdes [e], Jose Ignacio Priego-Quesada [f], Alejandro Weinstein [d], Oscar Valencia [d,g], Marcos R Kunzler [a], Joel Alvarez-Ruf [h,i], Felipe P Carpes [a,*]

[a] Laboratory of Neuromechanics, Universidade Federal do Pampa, Uruguaiana, Brazil
[b] Carrera de Kinesiología, Departamento de Cs. de la Salud, Facultad de Medicina, Pontificia Universidad Católica, Santiago, Chile
[c] Clinica MEDS, Santiago, Chile
[d] Centro de Investigación y Desarrollo en Ingeniería en Salud, Universidad de Valparaíso, Chile
[e] School of Sport, Exercise and Rehabilitation Sciences, Centre of Precision Rehabilitation for Spinal Pain (CPR Spine), College of Life and Environmental Sciences, University of Birmingham, Birmingham, United Kingdom
[f] Department of Physical Education and Sport, Research Group in Sport Biomechanics, University of Valencia, Valencia, Spain
[g] Laboratorio LIBFE. Escuela de Kinesiología. Universidad de los Andes, Santiago, Chile
[h] Laboratorio de Cognición y Comportamiento Sensoriomotor, Departamento de Kinesiología, Universidad Metropolitana de Ciencias de la Educación, Santiago, Chile
[i] Laboratorio de Biomecánica Clínica, Facultad de Medicina Clínica Alemana, Universidad del Desarrollo, Carrera de Kinesiología, Santiago, Chile

ARTICLE INFO

Keywords:
Electromyography
Methods
Muscle activation
Fourier
Gastrocnemius medialis
Fatigue

ABSTRACT

The Short-Time Fourier transform (STFT) is a helpful tool to identify muscle fatigue with clinical and sports applications. However, the choice of STFT parameters may affect the estimation of myoelectrical manifestations of fatigue. Here, we determine the effect of window length and overlap selections on the frequency slope and the coefficient of variation from EMG spectrum features in fatiguing contractions. We also determine whether STFT parameters affect the relationship between frequency slopes and task failure. Eighty-eight healthy adult men performed one-leg heel-rise until exhaustion. A factorial design with a window length of 50, 100, 250, 500, and 1000 ms with 0, 25, 50, 75, and 90% of overlap was used. The frequency slope was non-linearly fitted as a task failure function, followed by a dimensionality reduction and clustering analysis. The STFT parameters elicited five patterns. A small window length produced a higher slope frequency for the peak frequency ($p < 0.001$). The contrary was found for the mean and median frequency ($p < 0.001$). A larger window length elicited a higher slope frequency for the mean and peak frequencies. The largest frequency slope and dispersion was found for a window length of 50 ms without overlap using peak frequency. A combination of 250 ms with 50% of overlap reduced the dispersion both for peak, median, and mean frequency, but decreased the slope frequency. Therefore, the selection of STFT parameters during dynamic contractions should be accompanied by a mechanical measure of the task failure, and its parameters should be adjusted according to the experiment's requirements.

1. Introduction

Muscle fatigue is characterized by reducing the maximal capacity to generate force or power output (Vøllestad, 1997). It can be assessed by reductions in maximal force or time until task failure (Enoka and Duchateau, 2008). Although these assessments provide information when fatigue is installed, evaluating changes in muscle's electrophysiological properties extracted from electromyography time-series helps identify fatigue or non-fatigue status (Merletti et al., 1990). The myoelectric manifestations of muscle fatigue are indirectly related to reduced motor unit firing rate (Mettler and Griffin, 2016) and a concomitant decrease in muscle fiber conduction velocity (Rampichini et al., 2020). This information can be obtained by analyzing different spectral Short-Time Fourier Transform (STFT) patterns (Karthick et al.,

* Corresponding author at: Address: Laboratory of Neuromechanics, Universidade Federal do Pampa, Uruguaiana, Brazil.
E-mail address: carpes@unipampa.edu.br (F.P. Carpes).

https://doi.org/10.1016/j.jbiomech.2021.110598
Accepted 24 June 2021
Available online 29 June 2021

2016).

The variation in the EMG spectrum as a function of time can be estimated by applying the Fourier transform to signal segments. The multiple sequences of Fourier transform extracted from a signal is known as the STFT (Cifrek et al., 2009; Jeon et al., 2020). The STFT provides time-localized frequency information of how the frequency components of a signal vary over time. The signal segments, also known as window length, affect the time and frequency resolution of the STFT. An increase in the widow length increases the frequency resolution and decreases the time resolution. Meanwhile, a decrease in the window length decreases the frequency resolution and increases the time resolution (Jeon et al., 2020). Therefore, the STFT is widely used for frequency tracking over time (Zhang et al., 2020), and it is of particular interest in assessing biological signals and supporting decisions between fatigue or no-fatigue status (Cifrek et al., 2009; Rampichini et al., 2020). The relatively low computational cost allows the easy implementation of detection algorithms, i.e., features extraction are used to detect several conditions using machine learning algorithms (Wang et al., 2018b).

The features median, mean, and peak frequencies extracted from the electromyography periodogram are commonly used to quantify the myoelectric manifestations of muscle fatigue (Cifrek et al., 2009, 2000; Merletti et al., 1990; Rampichini et al., 2020; Shair et al., 2017). These descriptors estimate the changes in the sum of motor units action potential trains (MUAPT) in response to fatigue when the spectrum shifts towards lower frequencies (Cifrek et al., 2009, 2000; Eken et al., 2019; Martinez-Valdes et al., 2016; Rampichini et al., 2020). Applying regressions methods to the myoelectric manifestations of muscle fatigue frequency parameters over time allows determining the frequency slope during a muscle contraction (rate of change of frequency in time) (Merletti et al., 1990). More negative slopes represent a larger left shifting of the spectrum (also known as compression of the spectrum), which is associated with higher muscle fatigue status (Ament et al., 1993; Cifrek et al., 2009, 2000; Eken et al., 2019; Merletti et al., 1990). However, this approach has limitations due to the low sensitivity for the motor unit's discharge rate (Rampichini et al., 2020), EMG amplitude cancelation (Cifrek et al., 2009; Rampichini et al., 2020), frequency leakage (Tan and Jiang, 2019), and time–frequency resolution problems. The STFT time–frequency resolution limitations can be overcome by using more modern methods such as wavelets (Cifrek et al., 2009; Costa et al., 2010; Waly et al., 1996). However, physiological information is available in the periodograms to be used for muscle fatigue (Costa et al., 2010). Previous studies using bipolar and high-density EMG recordings found high variability in the chosen window length for analysis of isometric and dynamic contractions (Ament et al., 1993; Angelova et al., 2018; Cifrek et al., 2009, 2000; do Espírito Santo et al., 2018; Falla et al., 2017; Guzmán-Venegas et al., 2015; Hawkes et al., 2018; Hegyi et al., 2019; Hill et al., 2018; Jordanic et al., 2016; Jordanić et al., 2017; Watanabe et al., 2018; Zhu et al., 2017). Most of these studies did not provide details about the windows overlap (do Espírito Santo et al., 2018; Hawkes et al., 2018; Hill et al., 2018; Lark et al., 2019). Furthermore, the effects of window length and overlap have mainly been studied for isometric contractions (Xie and Wang, 2006; Zhang et al., 2010), but its effects remain unclear for dynamic muscle contractions. The recognition of adequate parameters is essential to avoid bias (Jordanic et al., 2016; Waly et al., 1996). Most importantly, these parameters must accurately predict failure during dynamic fatiguing tasks (Cifrek et al., 2009). However, an improper selection of window length and overlap might worse the sensitivity of EMG parameters to assess fatigue during dynamic contractions.

Continuous wavelet transform and STFT can provide similar muscle fatigue estimations, but considerably higher variability is found for STFT outcomes (Costa et al., 2010). Hence, we hypothesized that only a subset of the STFT parameters allows estimating muscle fatigue robustly. Recently, dimensionaity reduction technique, known as Uniform Manifold Approximation and Projection (UMAP), combined with density-based spatial clustering of applications with noise (DBSCAN) technique has been successfully used to find latent information of raw data (McInnes et al., 2018). For this reason, we considered that these techniques might be helpful to understand the effect of STFT on the estimation of muscle fatigue. Also, considering that the gastrocnemius medialis muscle is highly susceptible to fatigue during dynamic contractions (Ament et al., 1993), we selected this muscle as a appropriate model to investigate the effects of the STFT parameters on surface EMG outcomes in response to muscle fatigue. Therefore, here we aimed to determine the effects of STFT window length and overlap parameters on the frequency slope and coefficient of variation from median, mean, and peak frequencies from EMG data from the gastrocnemius medialis recorded during a fatiguing protocol until task failure. We also determine which clusters of STFT parameters affect the relationship between the frequency slope and task failure.

2. Material and methods

2.1. Study design

The study had two factors (window length and overlap) and five levels for window length (50, 100, 250, 500, and 1000 ms) and overlap (0, 25, 50, 75, and 90%). The sample included 88 healthy untrained men of age 22 ± 2 years, height 172.4 ± 2.5 cm, and body mass 71 ± 6 kg. The eligible participants were male adults, university students, with ages between 18 and 25 years old, and not enrolled in regular physical activity. They were self-reported as healthy, without a life history of injury to the lower extremities, no history of cardiovascular or metabolic alterations, no skin allergy, chronic pain, or cognitive impairments. Participants were requested to avoid alcohol intake and perform any physical exercise and keep their regular daily routine 48 h before the experiment. Any participant was excluded if they reported alcohol intake, physical exercise, or sleep alteration in the night before the experiment. This study was approved by the local institutional ethics committee IRB 23032019. All participants signed an informed consent form, agreeing to participate in the study.

2.2. Sample size

A sample size of 80 participants was *a priori* estimated considering a difference for factorial ANOVA with two factors (window length and overlap) and five levels for each one, using the F-test family distribution, an alpha error of 5%, the statistical power of 80% (four times the alpha error). We considered that the EMG differences could require a small (0.01) to medium effect size (0.06) due to intrinsical variability and decided for an arbitrary η^2 of 0.025. Furthermore, eight additional participants were included to anticipate possible losses (10% of estimation). The sample size estimation was performed using G*Power software version 3.1.9.2 (Kiel University, Germany).

2.3. Fatigue protocol

Participants performed the one-leg heel-rise test on a plane surface until exhaustion (Fig. 1). During the test, they were allowed to touch two fingers over the wall to help keep the balance (De la Fuente et al., 2018). Each participant was familiarized with the task one week before data collection. For data collection, after performing a 10 min warm-up pedaling at 60 rpm on a cycle ergometer (535U, SportsArt, USA) without external load, the participants performed the one-leg heel-rise test. They continuously lifted their heels as high as possible at a rhythm of 45 bpm following auditory feedback provided by a metronome (Google, USA). Task failure was defined as the point where participants could no longer lift the heel. Constant visual supervision and verbal encouragement were given to each participant to control the heel's lift. The criteria to finish the test was the drop of the cadence or the exhaustion of volunteers, defined as the incapacity to lift the heel from the floor.

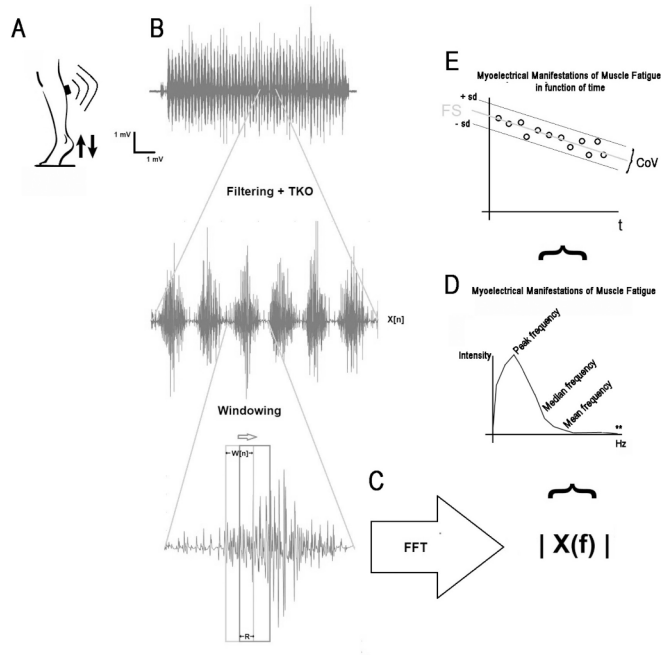

Fig. 1. Experiment design. A. The figure shows the heel-rise test until task failure where the time series of the electromyography signal (x [n]) is wirelessly transmitted, collected to be zero mean centered, and filtered. B. Then, each burst is identified using the Taeger-Keiser Operator (TKO). On each burst, a window manipulation of the length and the overlap (R) of the window (w [n]) is performed. C. From each segmented signal, the Fast Fourier Transform (FFT) is applied, and the magnitude is obtained. D. From each segmented signal, the frequency features mean, median, and peak can be extracted from spectrum, ** notice that if the sample frequency increase the median and mean frequencies displaces towards right frequencies (right-skewed distribution). E. Finally, the frequency slope (FS) is extracted from linear regression, and the dispersion of data measured as the coefficient of variance (CoV) also is obtained. sd = standard deviation.

2.4. Data acquisition and processing

Muscle activation was recorded continuously during the performance of the one-leg heel-rise test by a wireless EMG sensor placed on the skin over the gastrocnemius medialis (Delsys inc., USA). The skin was shaved and cleaned with alcohol before the electrode placement according to SENIAM guidelines (Hermens et al., 2000). The EMG signals were acquired using a Trigno^{TM} electromyography amplifier (Delsys Inc., Boston, USA) with an Avanti sensor (Delsys Inc., Boston, USA) with an inter-electrode distance of 10 mm (De Luca et al., 2012). Data were collected with a 16-bit analog–digital converter card (Vicon Motion Systems, Oxford, UK) and sampled at 4 kHz, analog bandpass filtered (20 ± 5–450 ± 50 Hz), CMRR > 80 dB, resolution of 168 nV/bit, basal noise of < 0.75 μV, with hardware amplification of 1000 V/V. All data were recorded using the software Nexus 2.0 (Vicon Motion Systems, Oxford, UK).

2.5. Data processing and analysis

The EMG signals were zero mean-centered, zero-padded to equal the length of the window used. They were filtered by a zero-lag fourth-order bandpass Butterworth filter with a bandpass between 20 and 450 Hz. The Teager-Kaiser energy operator threshold-based method was used to detect the individual EMG muscle contractions bursts during the heel test (Solnik et al., 2010), see Fig. 1. This operator is defined as $\Psi[x[n]] = x[n]^2 - x[n+1]x[n-1]$, where the $x[n]$ is a time series at sample n. Rest EMG signals used for the Kaiser energy operator threshold-based were extracted while standing and analyzed for 500 ms.

The STFT provides time-localized frequency information when frequency components of a signal vary over time (Jeon et al., 2020; Karthick et al., 2016). The discrete-time form of the STFT was defined as $X_{(m,\omega)} = \sum_{n=-\infty}^{\infty} x[n]w[n-mR]e^{-j\omega n}$. The STFT was evaluated at sample time m, $x[n]$ was each EMG burst time-series at sample time n, $w[n]$ was a rectangular window function, and R was the hop size that determines the amount of overlap. The window length used were 50, 100, 250, 500, and 1000 ms. The overlap, R, was 0, 25, 50, 75, and 90% (Fig. 1). Although there are many options for selecting the shape of the window function, we used a rectangular one as a fixed and controlled experimental factor. The effect of the window type on myoelectric manifestations of fatigue is outside the scope of our study, and these limitations have been addressed in a previous publication (Tan and Jiang, 2019). Finally, as $X_{(m,\omega)}$ is a complex quantity, the assessment of fatigue was performed using the STFT's magnitude$|X_{(m,\omega)}|$ (Karthick et al., 2016). As a result, a Fourier transformation was determined for each contraction burst, which allowed the extraction of median, mean, and peak frequencies (frequency features) from each spectrum varying the length of $w[n]$ and R, see Fig. 1.

The three frequency features combined with the five window lengths and the five overlaps resulted in 75 time series containing a variation of the median, mean, and peak frequencies obtained from each EMG burst (Fig. 1). We applied a linear regression to estimate the rate of change in frequency (Hz s^{-1}) during the motor task (Horita and Ishiko, 1987; Priego-Quesada et al., 2019), see Fig. 1. From the same 75 time series, the coefficient of variation, defined as the ratio between standard deviation and mean and expressed as a percentage, was obtained for each frequency feature.

To find the window length and overlap that minimizes the over- and sub-estimation (outliers) of the coefficient of variation and frequency slope, we estimated the centroid of the plane formed by the ratio between the frequency slopes and the coefficient of variation. This ratio reflects the capability to estimate the variation of a frequency feature over the time normalized by its dispersion. The centroid was the sum of the dot product between the ratio of the frequency slope/ coefficient of variation and the factor level (1, 2, 3, 4, or 5), divided by the total sum of the ratio of the frequency slope/ coefficient of variation, expressed as the number of window and overlap (Jordanic et al., 2016).

Finally, to understand the sensitivity to the task failure for all combinations of window length and overlap, we obtained curve patterns from the relationship between the frequency slope and the number of heel rise repetitions until task failure. These patterns were fitted using the non-linear least squared method with the model $y = ae^{bx} + ce^{dx}$, where y is the frequency slope for each combination of window length, overlap, and frequency features (a total of 75 models), x is the number of repetitions until task failure for each participant, and a, b, c, and d are model parameters (Merletti et al., 1990). Hence, one curve was fitted for each combination of window length, overlap, and frequency features. Therefore, if a homogeneous curve pattern for all combinations exists, there will be only one pattern. In contrast, if different patterns exist, different combinations would produce different patterns from the same sample.

All computations were performed using Matlab 2020a software (Matworks Inc., USA) and its signal processing toolbox including the functions fft, next2power, filtfit, and butter. We also used basic math functions like image, surf, abs, linspace, median, fix, size, find, sum, polyfit, std, mean, repmat, and exp. The non-linear fitting was made through the curve fitting tool available on the app matlab screen to perform the non-linear model previously described.

2.6. Non-linear dimensionality reduction and clustering

We performed a non-linear dimensionality reduction to capture the latent data characteristics using the UMAP algorithm (McInnes et al., 2018). It determined the pattern from the relationship between the

frequency slope and the heel-rise repetitions until failure for all parameters, features, and participants. The UMAP approximates a high-dimensional dataset (all relationships between the slope and the number of heel rise repetitions until failure) by a low dimensional dataset (a projection of the raw data from a Riemannian manifold to a space of the Real numbers, which we could easily refers as the UMAP domain) by creating a fuzzy topological structure using the gradient of the binary cross-entropy as the loss function. The weights are the probability of the existence of 0-simplex (lowest dimensional connection) or 1-simplex, which is a topographic representation of the connection between neighbors (McInnes et al., 2018). The weight between neighbors was modeled as $w = e^{-d(x_i - x_j) - \rho_i/\sigma}$, being ρ_i the distance from i-th data points to its first nearest neighbor (Oskolkov, 2019). The binary cross-entropy was modeled as $\sum_{je\in E}\left[w_h(e)\log(\frac{W_h(e)}{W_i(e)}) + (1 - w_h(e))\log(\frac{1-W_h(e)}{1-W_i(e)})\right]$. The input to UMAP was the set of 75 combinations, each one represented by the fitted curve evaluated for x between 1 and 88, that is a time series that involved a dimension of 88 heel rises until task failure. The algorithm reduced these 75 curves of dimension 88 into 75 points of dimension 3 into the UMAP domain. The parameters used for the UMAP algorithm were: Euclidean metric, number of neighbors set to 7, learning rate set to 1, local connectivity set to 1, repulsion strength set to 1, and minimal distance equal 0.5 (Meehan et al., 2020).

DBSCAN was used after dimensionality reduction steps described in the previous paragraph. Each DBSCAN cluster represents a set of STFT parameters that produces a similar muscle fatigue model performed in the UMAP domain grouping dataset based on the density of the space. Then, we determined the clusters or families of parameters related to its capacity to identify muscle fatigue, and labeled the families of the pattern (clusters). The parameter for DBSCAN was an epsilon set to 5. Finally, the mean of the data was used to summarize the behavior for each cluster. The estimations were obtained using the Matlab 2020a software (Mathworks, Inc., USA).

2.7. Outcomes

The study outcomes were the frequency slope (Hz s^{-1}) and the coefficient of variability (%) for the 75 possible combinations of STFT parameters, the number of heel-rise repetitions to failure, the clusters of STFT parameters (label of the cluster), and the patterns obtained from the relationship between the frequency slope and task failure (Hz s^{-1} no. of repetitions^{-1}).

2.8. Statistic analysis

Results are described as mean, standard deviation, percentage, proportions, and coefficients. The Shapiro-Wilk test confirmed the normality of data distribution. Homoscedasticity and sphericity assumptions were confirmed using the Bartlett and Mauchly tests, respectively. To determine the within and between groups effects and interactions, we conducted a two-way ANOVA with five levels for window length (50, 100, 250, 500, and 1000 ms), and five levels for overlap (0, 25, 50, 75, and 90%) with a Bonferroni post-hoc test, considering a significance level set at 0.05. The proportion between myoelectric manifestations for each cluster was obtained using an adjusted-χ^2 test with confidence of 99%, 10 K samples for Monte Carlo simulation, and 0.5 references of the proportions. To compare proportions, we used the Pearson's-χ^2 test for a contingency table of 3 × 5. All data were analyzed considering a significance level set at 0.05 using the trial SPSS software (IBM, USA).

3. Results

Window length showed a main effect on the frequency slope and the coefficient of variation ($p < 0.001$, Fig. 2). The multiple comparisons showed that the smaller window lengths (50, 100, and 250 ms) elicited larger frequency slopes for peak frequency ($p < 0.001$) while larger window lengths (1000 and 500 ms) elicited larger frequency slopes in the median frequency ($p < 0.001$). Similarly, the largest window length (1000 ms) elicited larger frequency slopes for mean frequency ($p < 0.001$). The multiple comparisons showed that the smaller window length (50 and 100 ms) elicited a small coefficient of variation for peak frequency ($p < 0.001$). The larger window lengths (500 and 1000 ms) elicited the smaller coefficient of variation in the median frequency ($p < 0.001$). The smaller window lengths (50, 100, and 250 ms) elicited the smaller coefficient of variance for mean frequency ($p < 0.001$).

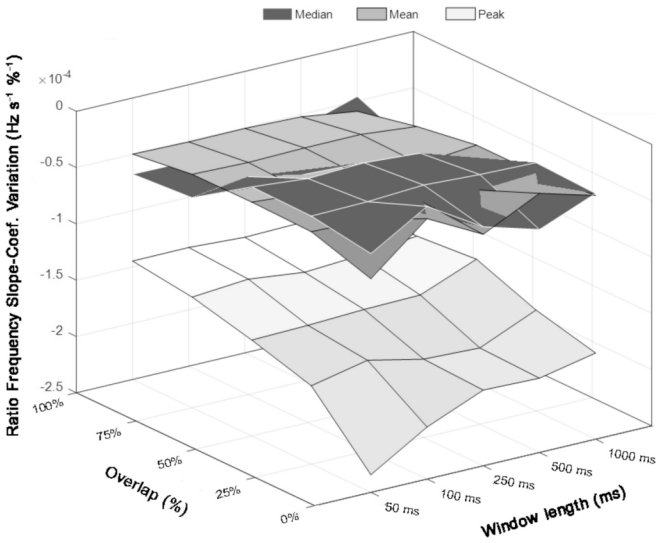

Fig. 2. STFT parameters behavior during the heel-rise test. The figure shows how the frequency slope obtained by linear regression and normalized respect for its dispersion behaves regarding the window length and overlap for the mean, median, and peak frequency. Main effects for window length ($p < 0.0001$), overlap ($p < 0.0001$), and interaction between have existed ($p < 0.0001$). The lowest value was found for the combination of 50 ms and overlap of 0% using the peak frequency, and the centroid for the three planes is located at 250 ms with 50% of overlap. For the same motor task performed until exhaustion, different manifestations of muscle fatigue depending on STFT parameters existed.

Overlap showed a main effect for the coefficient of variation ($p < 0.001$, Fig. 2), but no effect was found for frequency slope ($p = 0.1584$). The multiple comparisons showed that the smaller overlap (0%) elicited the smaller coefficient of variation for peak frequency ($p < 0.001$). The overlap of 25% elicited a small coefficient of variation for peak frequency ($p < 0.001$). The smaller overlap (0%) elicited the smaller coefficient of variation for mean frequency ($p < 0.001$). Interaction between window length and overlap was found for the coefficient of variation ($p < 0.001$) and frequency slope ($p < 0.001$).

A 50 ms window length without overlap (0%) resulted in the minimal value for the plane 'frequency slope - coefficient of variation' (Fig. 2). A 250 ms window length and a 50% overlap were the nearest parameters to the location of the centroids for the plane 'frequency slope - coefficient of variation' (Table 1).

Task failure occurred after 39.6 ± 13.3 heel-rise repetitions (median 45; range 18 to 63 repetitions). The R-squares for the relationship between the frequency slope and the number of heel rise repetitions until

Table 1
Centroids localization in the coefficient of variation – slope frequency plane.

	(Windows coordinate, Overlap coordinate)
Median frequencyMean frequencyPeak frequency	(3.39, 3.03)(3.09, 2.96)(2.79, 2.92)

failure are summarized in Table 2. There were 5 clusters of STFT parameters detected by DBSCAN in the UMAP domain. (Fig. 3 and Table 2). The bigger cluster that includes higher slope frequencies was found for the fifth cluster (Fig. 3 and Table 2). The frequency features corresponding to each cluster are described in Table 3. The relationship between the frequency slope and task failure patterns is summarized in Fig. 3.

4. Discussion

Here, we show that the selection of STFT parameters affects the frequency slope of myoelectrical manifestations of fatigue estimated from the median, mean, and peak frequencies recorded from gastrocnemius medialis. This, in turn, affects the sensitivity of muscle fatigue estimation. The window length and overlap directly influenced the relationship between slope frequency and task failure, distorting different myoelectrical manifestations of muscle fatigue depending on the parameters selected for the STFT.

The endurance capacity varied among the participants, most likely due to different levels of neuromuscular adaptations to fatigue between the individuals (Walton et al., 2002). An early or delayed task failure may depend on participant tolerance to fatigue. This helps to understand the different sensitivity patterns for the relationship between slope frequency and task failure. In particular, the fitted series in each cluster with different frequency slopes and dispersion demonstrates how the STFT parameters change the frequency manifestation of muscle fatigue. For instance, some clusters show a higher electrical frequency slope for an earlier task failure, such as cluster 1 showed. This cluster appears to be physiological consistent with individuals with poor tolerance to fatigue (higher electrical frequency slope for an earlier task failure) and with individuals showing better tolerance to fatigue (negative frequency slope, but lower for a delayed task failure). The pattern was not observed in all clusters. For example, cluster 5 showed a lower frequency slope for an earlier task failure in comparison with delayed task failure, but this cluster achieved the highest slope frequencies compared to the the clusters. This suggests that STFT parameters may introduce non-linear distortion in the electrical manifestation of fatigue.

Here, we found that a window length of 50 ms with 0% overlap of the peak frequency resulted in a higher frequency slope. However, it is essential to consider that a small window length elicits a high risk of overestimating muscle fatigue when the peak frequency is used. In contrast, a large length windows had the opposing effect. This confusion may result from noise (outliers) that increase the dispersion and affect the regression outcomes. Hence, we recommended treating the outliers before applying the regression, especially for the peak frequency. If it is decided to use the mean and median frequencies extracted from raw signals highly sampled, a decision of the band for analysis should be considered because the mean and median are sensitive to a right displacement in a right-skewness distribution of frequencies losing sensitivity to muscle fatigue. STFT parameters may easily influence frequency slopes, but it is worthy to mention that the frequency slope per se does not reflect the entire fatigue process (Ament et al., 1993; González-Izal et al., 2010; Horita and Ishiko, 1987; Wang et al., 2018a). Frequency slopes mainly reflect the global electrophysiological processes accompanying the generation of fatigue, which depends on

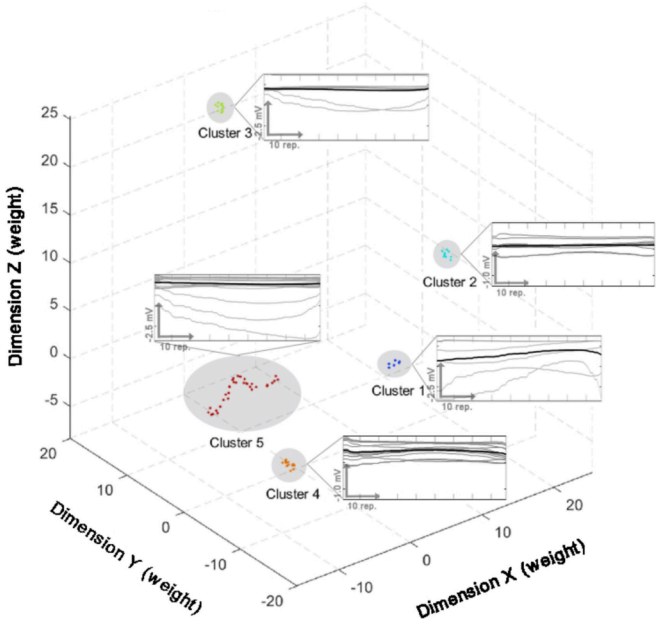

Fig. 3. Non-linear dimensionality reduction and clustering for the relationship between slope frequency and task failure (number of maximal heel rises obtained by the sample). The figure shows the projection of the UMAP algorithm into a tridimensional domain measured in weights. The dots indicate the projected families of STFT parameters, and the gray ellipsoid shadow delimits the recognized cluster by DBSCAN algorithm. Each dot cluster is expanded, showing the pattern of sensitivity to task failure as graphs; the black line of these graphs illustrates the cluster's mean pattern.

Table 3
Family parameters.

	Median frequency				
	50 ms	100 ms	250 ms	500 ms	1000 ms
90%	3	3	3	3	3
75%	3	3	3	3	3
50%	2	2	2	2	2
25%	1	1	2	2	2
0%	1	1	1	1	1
	Mean frequency				
	50 ms	100 ms	250 ms	500 ms	1000 ms
90%	5	5	5	5	5
75%	4	5	5	5	5
50%	4	4	4	4	4
25%	4	4	4	4	4
0%	3	3	3	4	4
	Peak frequency				
	50 ms	100 ms	250 ms	500 ms	1000 ms
90%	5	5	5	5	5
75%	5	5	5	5	5
50%	5	5	5	5	5
25%	5	5	5	5	5
0%	5	5	5	5	5

Table 2
Proportion of windows and overlap combinations found in the 5 clusters and its goodness-of-fit statistics.

Cluster	Cluster 1	Cluster 2	Cluster 3	Cluster 4	Cluster 5
Median frequencyMean frequencyPeak frequencyTotalAdjusted- χ^2	28% (7/25)0% (0/25) 0% (0/25)9.3% (7/75) $p < 0.001$	36% (9/25)0% (0/25) 0% (0/25)12% (9/75) $p < 0.001$	36% (9/25)12% (3/25) 0% (0/25)16% (12/75) $p < 0.001$	0% (0/25)52% (13/25) 0% (0/25)17.3% (13/75)$p < 0.001$	0% (0/25)36% (9/25) 100% (25/25)45.3% (34/75)$p < 0.001$
erson- χ^2 : $p < 0.001$					
Goodness-of-fit:	Cluster 1	Cluster 2	Cluster 3	Cluster 4	Cluster 5
R-square	0.57 ± 0.28	0.51 ± 0.25	0.36 ± 0.22	0.38 ± 0.25	0.46 ± 0.24

central and peripheral motor unit properties. However, these properties may be hidden by synthetic assumptions, such as we showed here, that affects the frequency slope. Moreover, non-physiological phenomena from the target muscle, such as cross-talk and volume conduction, may also influence the frequency slope (Farina et al., 2014). Therefore, the use of the frequency slope as an index of fatigue requires caution.

Fourier methods have been validated to analyze EMG signals when slow changes exist in the time domain (Farina et al., 2014; Srhoj-Egekher et al., 2011). Nevertheless, some complexities related to muscle fatigue, such as motor unit action potential changes in morphology, amplitude and/or spatial distribution, can influence spectral analysis (Martinez-Valdes et al., 2020). Indeed, these complexities can affect both time and spectrum domain characteristics (Rampichini et al., 2020), which may lead to misinterpretation of the physiological phenomenon due to fixed resolution problems (Cifrek et al., 2009; Singh et al., 2017; Srhoj-Egekher et al., 2011). In these cases, wavelets are suggested by its adaptative time–frequency resolution (Costa et al., 2010). However, Fourier decomposition methods generating a set of a small number of bands derived from empirical decomposition mode have been proposed as a better method for non-linear behavior than STFT or wavelet method (Singh et al., 2017). Nevertheless, more deep work might be required to understand and develop better techniques that might help dynamic muscle fatigue.

When we compared window lengths of 50 ms, 100 ms, and 250 ms, the largest slopes were found when the peak frequency was considered. In contrast, the mean and median frequencies generated the highest frequency slope, with windows of 500 ms and 1000 ms. This suggests a negative covariance between the frequency components and the number of heel-rise repetitions, explaining the largest negative frequency slope obtained after the linear regression analysis (Cifrek et al., 2009). An improper parameter definition may result in statistical bias. For instance, the statistical type I error is induced when contractions are not performed to fatigue, and a negative frequency slope is found (Krzywinski and Altman, 2013). On the other hand, considering that the median and mean frequencies show small frequency slopes, this could be associated with an under-estimation, resulting in a higher probability of statistical type II error (Krzywinski and Altman, 2013).

The largest dispersion found for the peak frequency is in agreement with a previous report (Srhoj-Egekher et al., 2011) and expressed a large spread of data with respect to the mean and median frequencies. This behavior also means that the sum of squares is large. Therefore, to avoid the statistical type II error when the peak frequency is used, a larger number of samples is needed, compared to the mean and median frequencies (Krzywinski and Altman, 2013). Peak frequency may be affected by a small number of samples, despite its better capacity to generate a more negative frequency slope.

Larger overlap increased dispersion of data for peak and mean frequencies. Median and peak frequencies showed similar behavior, except for the 0% overlap showing the highest dispersion. As we discussed for selecting window length, we need to be careful with the sample size to avoid statistical type II error due to increased data dispersion (Krzywinski and Altman, 2013). Finally, the centroid method used here tends to smooth small or large values in the intensity-dispersion plane, acting as a low-pass filter. However, this does not guarantee the best sensitivity to predict task failure, being the 250 ms with 50% considered a conservative selection of parameters.

We acknowledge the limitation of windowing and overlapping being set only in a forward manner. Another limitation was our incapacity to consider metabolic markers of peripheral fatigue to estimate fatigue intensity and correlate them with different stationary parameters from the EMG signals.

5. Conclusions

A window length of 50 ms without overlap using peak frequency provides the highest frequency slope but generates a large dispersion of data. Instead, a 250 ms window length with 50% of overlap for the mean, median, and peak frequency reduce the data dispersion but decreases the frequency slope during dynamic contractions. Therefore, we recommend that the selection of STFT parameters during dynamic contractions to be accompanied by a mechanical measure of the task failure. The STFT parameters should be adjusted according to the experiment's requirements.

Funding

CD was supported by the De Luca Foundation and Delsys Inc. through Delsys' donation initiative 2020. FPC is supported by a CNPq research fellowship. AW was supported by grant BASAL FB0008. OV was supported by Fondo de Ayuda a la Investigación, Universidad de los Andes, Santiago, Chile (FAI: INV-IN-2017-01).

CRediT authorship contribution statement

Carlos De Fuente: Conceptualization, Data curation, Formal analysis, Funding acquisition, Investigation, Methodology, Project administration, Resources, Software, Supervision, Validation, Visualization, Writing - original draft, Writing - review & editing. **Eduardo Martinez-Valdes:** Conceptualization, Formal analysis, Methodology, Supervision, Validation, Visualization, Writing - original draft, Writing - review & editing. **Jose Ignacio Priego-Quesada:** Formal analysis, Methodology, Validation, Visualization, Writing - original draft, Writing - review & editing. **Alejandro Weinstein:** Conceptualization, Formal analysis, Funding acquisition, Investigation, Methodology, Project administration, Supervision, Validation, Visualization, Writing - original draft, Writing - review & editing. **Oscar Valencia:** Formal analysis, Methodology, Validation, Visualization, Writing - original draft, Writing - review & editing. **Marcos R Kunzler:** Formal analysis, Methodology, Validation, Visualization, Writing - original draft, Writing - review & editing. **Joel Alvarez-Ruf:** Conceptualization, Formal analysis, Methodology, Supervision, Validation, Visualization, Writing - original draft, Writing - review & editing. **Felipe P Carpes:** Conceptualization, Formal analysis, Funding acquisition, Investigation, Methodology, Project administration, Supervision, Validation, Visualization, Writing - original draft, Writing - review & editing.

Declaration of Competing Interest

The authors declare that they have no known competing financial interests or personal relationships that could have appeared to influence the work reported in this paper.

References

Ament, W., Bonga, G.J., Hof, A.L., Verkerke, G.J., 1993. EMG median power frequency in an exhausting exercise. J. Electromyogr. Kinesiol. 3, 214–220. https://doi.org/10.1016/1050-6411(93)90010-T.

Angelova, S., Ribagin, S., Raikova, R., Veneva, I., 2018. Power frequency spectrum analysis of surface EMG signals of upper limb muscles during elbow flexion - A comparison between healthy subjects and stroke survivors. J. Electromyogr. Kinesiol. 38, 7–16. https://doi.org/10.1016/j.jelekin.2017.10.013.

Cifrek, M., Medved, V., Tonković, S., Ostojić, S., 2009. Surface EMG based muscle fatigue evaluation in biomechanics. Clin. Biomech. (Bristol, Avon) 24, 327–340. https://doi.org/10.1016/j.clinbiomech.2009.01.010.

Cifrek, M., Tonković, S., Medved, V., 2000. Measurement and analysis of surface myoelectric signals during fatigued cyclic dynamic contractions. Measurement 27, 85–92. https://doi.org/10.1016/S0263-2241(99)00059-7.

Costa, M.V., Pereira, L.A., Oliveira, R.S., Pedro, R.E., Camata, T.V., Abrao, T., Brunetto, M.A.C., Altimari, L.R., 2010. Fourier and wavelet spectral analysis of EMG signals in maximal constant load dynamic exercise. Annu. Int. Conf. IEEE Eng. Med. Biol. Soc. 2010, 4622–4625. https://doi.org/10.1109/IEMBS.2010.5626474.

De la Fuente, C., Cruz-Montecinos, C., De la Fuente, CJ, Peña y Lillo, R., Chamorro, C., Henriquez, H., 2018. Early short-term recovery of single-leg heel rise and ATRS after Achilles tenorrhaphy: Cluster analysis. Asian Journal of Sports Medicine 9, e67661. https://doi.org/10.5812/asjsm.67661.

De Luca, C.J., Kuznetsov, M., Gilmore, L.D., Roy, S.H., 2012. Inter-electrode spacing of surface EMG sensors: reduction of cross-talk contamination during voluntary

contractions. J. Biomech. 45, 555–561. https://doi.org/10.1016/j.jbiomech.2011.11.010.
do Espírito Santo, R.C., Pompermayer, M.G., Bini, R.R., Olszewski, V., Teixeira, E.G., Chakr, R., Xavier, R.M., Brenol, C.V., 2018. Neuromuscular fatigue is weakly associated with perception of fatigue and function in patients with rheumatoid arthritis. Rheumatol. Int. 38, 415–423. https://doi.org/10.1007/s00296-017-3894-z.
Eken, M.M., Braendvik, S.M., Bardal, E.M., Houdijk, H., Dallmeijer, A.J., Roeleveld, K., 2019. Lower limb muscle fatigue during walking in children with cerebral palsy. Dev. Med. Child Neurol. 61, 212–218. https://doi.org/10.1111/dmcn.14002.
Enoka, R.M., Duchateau, J., 2008. Muscle fatigue: what, why and how it influences muscle function. J. Physiol. 586, 11–23. https://doi.org/10.1113/jphysiol.2007.139477.
Falla, D., Cescon, C., Lindstroem, R., Barbero, M., 2017. Muscle Pain Induces a Shift of the Spatial Distribution of Upper Trapezius Muscle Activity During a Repetitive Task: A Mechanism for Perpetuation of Pain With Repetitive Activity? Clin. J. Pain 33, 1006–1013. https://doi.org/10.1097/AJP.0000000000000513.
Farina, D., Merletti, R., Enoka, R.M., 2014. The extraction of neural strategies from the surface EMG: an update. J. Appl. Physiol. 117, 1215–1230. https://doi.org/10.1152/japplphysiol.00162.2014.
González-Izal, M., Malanda, A., Navarro-Amézqueta, I., Gorostiaga, E.M., Mallor, F., Ibañez, J., Izquierdo, M., 2010. EMG spectral indices and muscle power fatigue during dynamic contractions. J. Electromyogr. Kinesiol. 20, 233–240. https://doi.org/10.1016/j.jelekin.2009.03.011.
Guzmán-Venegas, R.A., Biotti Picand, J.L., de la Rosa, F.J.B., 2015. Functional compartmentalization of the human superficial masseter muscle. PLoS ONE 10, e0116923. https://doi.org/10.1371/journal.pone.0116923.
Hawkes, D., Grant, M., McMahon, J., Horsley, I., Khaiyat, O., 2018. Can grip strength be used as a surrogate marker to monitor recovery from shoulder fatigue? J. Electromyogr. Kinesiol. 41, 139–146. https://doi.org/10.1016/j.jelekin.2018.06.002.
Hegyi, A., Csala, D., Péter, A., Finni, T., Cronin, N.J., 2019. High-density electromyography activity in various hamstring exercises. Scand. J. Med. Sci. Sports 29, 34–43. https://doi.org/10.1111/sms.13303.
Hermens, H.J., Freriks, B., Disselhorst-Klug, C., Rau, G., 2000. Development of recommendations for SEMG sensors and sensor placement procedures. J. Electromyogr. Kinesiol. 10, 361–374. https://doi.org/10.1016/s1050-6411(00)00027-4.
Hill, E.C., Housh, T.J., Smith, C.M., Keller, J.L., Schmidt, R.J., Johnson, G.O., 2018. Sex- and Mode-specific Responses to Eccentric Muscle Fatigue. Int. J. Sports Med. 39, 893–901. https://doi.org/10.1055/a-0664-0733.
Horita, T., Ishiko, T., 1987. Relationships between muscle lactate accumulation and surface EMG activities during isokinetic contractions in man. Eur. J. Appl. Physiol. Occup. Physiol. 56, 18–23. https://doi.org/10.1007/BF00696370.
Jeon, H., Jung, Yongchul, Lee, S., Jung, Yunho, 2020. Area-Efficient Short-Time Fourier Transform Processor for Time-Frequency Analysis of Non-Stationary Signals. Appl. Sci. 10, 7208. https://doi.org/10.3390/app10207208.
Jordanic, M., Rojas-Martínez, M., Mañanas, M.A., Alonso, J.F., 2016. Spatial distribution of HD-EMG improves identification of task and force in patients with incomplete spinal cord injury. J. Neuroeng. Rehabil. 13, 41. https://doi.org/10.1186/s12984-016-0151-8.
Jordanić, M., Rojas-Martínez, M., Mañanas, M.A., Alonso, J.F., Marateb, H.R., 2017. A Novel Spatial Feature for the Identification of Motor Tasks Using High-Density Electromyography. Sensors (Basel) 17. https://doi.org/10.3390/s17071597.
Karthick, P.A., Navaneethakrishna, M., Punitha, N., Fredo, A.R.J., Ramakrishnan, S., 2016. Analysis of muscle fatigue conditions using time-frequency images and GLCM features. Curr. Directions Biomed. Eng. 2, 483–487. https://doi.org/10.1515/cdbme-2016-0107.
Krzywinski, M., Altman, N., 2013. Power and sample size. Nat. Methods 10, 1139–1140. https://doi.org/10.1038/nmeth.2738.
Lark, S.D., Dickie, J.A., Faulkner, J.A., Barnes, M.J., 2019. Muscle activation and local muscular fatigue during a 12-minute rotational bridge. Sports Biomech. 18, 402–413. https://doi.org/10.1080/14763141.2018.1433870.
Martinez-Valdes, E., Guzman-Venegas, R.A., Silvestre, R.A., Macdonald, J.H., Falla, D., Araneda, O.F., Haichelis, D., 2016. Electromyographic adjustments during continuous and intermittent incremental fatiguing cycling. Scand. J. Med. Sci. Sports 26, 1273–1282. https://doi.org/10.1111/sms.12578.
Martinez-Valdes, E., Negro, F., Falla, D., Dideriksen, J.L., Heckman, C.J., Farina, D., 2020. Inability to increase the neural drive to muscle is associated with task failure during submaximal contractions. J. Neurophysiol. 124, 1110–1121. https://doi.org/10.1152/jn.00447.2020.
McInnes, L., Healy, J., Melville, J., 2018. UMAP: Uniform Manifold Approximation and Projection for Dimension Reduction. arXiv:1802.03426 [cs, stat].
Meehan, C., Meehan, S., Moore, W., 2020. Uniform Manifold Approximation and Projection (UMAP). MATLAB Central File Exchange. URL https://www.mathworks.com/matlabcentral/fileexchange/71902 (accessed 8.11.20).
Merletti, R., Knaflitz, M., De Luca, C.J., 1990. Myoelectric manifestations of fatigue in voluntary and electrically elicited contractions. J. Appl. Physiol. 69, 1810–1820. https://doi.org/10.1152/jappl.1990.69.5.1810.
Mettler, J.A., Griffin, L., 2016. Muscular endurance training and motor unit firing patterns during fatigue. Exp. Brain Res. 234, 267–276. https://doi.org/10.1007/s00221-015-4455-x.
Oskolkov, N., 2019. How Exactly UMAP Works. Medium. URL https://towardsdatascience.com/how-exactly-umap-works-13e3040e1668 (accessed 12.14.20).
Priego-Quesada, J.I., Oficial-Casado, F., Gandia-Soriano, A., Carpes, F.P., 2019. A preliminary investigation about the observation of regional skin temperatures following cumulative training loads in triathletes during training camp. J. Therm. Biol. 84, 431–438. https://doi.org/10.1016/j.jtherbio.2019.07.035.
Rampichini, S., Vieira, T.M., Castiglioni, P., Merati, G., 2020. Complexity Analysis of Surface Electromyography for Assessing the Myoelectric Manifestation of Muscle Fatigue: A Review. Entropy 22, 529. https://doi.org/10.3390/e22050529.
Shair, E.F., Ahmad, S.A., Marhaban, M.H., Mohd Tamrin, S.B., Abdullah, A.R., 2017. EMG Processing Based Measures of Fatigue Assessment during Manual Lifting. Biomed. Res. Int. https://doi.org/10.1155/2017/3937254.
Singh, P., Joshi, S.D., Patney, R.K., Saha, K., 2017. The Fourier decomposition method for non-linear and non-stationary time series analysis. Proceedings of the Royal Society A: Mathematical, Physical and Engineering Sciences 473, 20160871. https://doi.org/10.1098/rspa.2016.0871.
Solnik, S., Rider, P., Steinweg, K., DeVita, P., Hortobágyi, T., 2010. Teager-Kaiser energy operator signal conditioning improves EMG onset detection. Eur. J. Appl. Physiol. 110, 489–498. https://doi.org/10.1007/s00421-010-1521-8.
Srhoj-Egekher, V., Cifrek, M., Medved, V., 2011. The application of Hilbert-Huang transform in the analysis of muscle fatigue during cyclic dynamic contractions. Med. Biol. Eng. Comput. 49, 659–669. https://doi.org/10.1007/s11517-010-0718-7.
Tan, L., Jiang, J., 2019. Chapter 4 - Discrete Fourier Transform and Signal Spectrum. In: Tan, L., Jiang, J. (Eds.), Digital Signal Processing (Third Edition). Academic Press, pp. 91–142. https://doi.org/10.1016/B978-0-12-815071-9.00004-X.
Vøllestad, N.K., 1997. Measurement of human muscle fatigue. J. Neurosci. Methods 74, 219–227. https://doi.org/10.1016/s0165-0270(97)02251-6.
Walton, D.M., Kuchinad, R.A., Ivanova, T.D., Garland, J.S., 2002. Reflex inhibition during muscle fatigue in endurance-trained and sedentary individuals. Eur. J. Appl. Physiol. 87, 462–468. https://doi.org/10.1007/s00421-002-0670-9.
Waly, S.M., Asfour, S.S., Khalil, T.M., 1996. Effects of time windowing on the estimated EMG parameters. Comput. Ind. Eng. 31, 515–518. https://doi.org/10.1016/0360-8352(96)00188-x.
Wang, L., Wang, Y., Ma, A., Ma, G., Ye, Y., Li, R., Lu, T., 2018a. A Comparative Study of EMG Indices in Muscle Fatigue Evaluation Based on Grey Relational Analysis during All-Out Cycling Exercise. Biomed. Res. Int. 2018, 9341215. https://doi.org/10.1155/2018/9341215. PMID: 29850588; PMCID: PMC5926489.
Wang, Z., Cao, L., Zhang, Z., Gong, X., Sun, Y., Wang, H., 2018b. Short time Fourier transformation and deep neural networks for motor imagery brain computer interface recognition. Concurrency and Computation: Practice and Experience 30, e4413. https://doi.org/10.1002/cpe.4413.
Watanabe, K., Kouzaki, M., Ogawa, M., Akima, H., Moritani, T., 2018. Relationships between muscle strength and multi-channel surface EMG parameters in eighty-eight elderly. Eur. Rev. Aging Phys. Act 15, 3. https://doi.org/10.1186/s11556-018-0192-z.
Xie, H., Wang, Z., 2006. Mean frequency derived via Hilbert-Huang transform with application to fatigue EMG signal analysis. Comput. Methods Programs Biomed. 82, 114–120. https://doi.org/10.1016/j.cmpb.2006.02.009.
Zhang, K., Xu, G., Han, Z., Ma, K., Zheng, X., Chen, L., Duan, N., Zhang, S., 2020. Data Augmentation for Motor Imagery Signal Classification Based on a Hybrid Neural Network. Sensors (Basel) 20. https://doi.org/10.3390/s20164485.
Zhang, Z.G., Liu, H.T., Chan, S.C., Luk, K.D.K., Hu, Y., 2010. Time-dependent power spectral density estimation of surface electromyography during isometric muscle contraction: methods and comparisons. J. Electromyogr. Kinesiol. 20, 89–101. https://doi.org/10.1016/j.jelekin.2008.09.007.
Zhu, M., Yu, B., Yang, W., Jiang, Y., Lu, L., Huang, Z., Chen, S., Li, G., 2017. Evaluation of normal swallowing functions by using dynamic high-density surface electromyography maps. Biomed. Eng. Online 16, 133. https://doi.org/10.1186/s12938-017-0424-x.